

# C–O-Bond Cleavage of Esters with a Naphthyl Group in the Higher Triplet Excited State during Two-Color Two-Laser Flash Photolysis

Xichen Cai,<sup>[a]</sup> Masanori Sakamoto,<sup>[a]</sup> Minoru Yamaji,<sup>[b]</sup> Mamoru Fujitsuka,<sup>[a]</sup> and Tetsuro Majima\*<sup>[a]</sup>

**Abstract:** A C–O-bond cleavage of esters having a naphthyl group, NpCO-OR and RCO-ONp (Np =  $\alpha$ - and  $\beta$ -naphthyl ( $^{\alpha}$ Np and  $^{\beta}$ Np, respectively), R = Ph and Me), was found during the two-color two-laser flash photolysis in acetonitrile. The C–O-bond cleavage occurred when NpCO-OR and RCO-ONp were excited to the singlet excited states ( $S_1$ ). On the other hand, no reaction occurred from the lowest triplet excited states ( $T_1$ ). When NpCO-OR( $T_1$ ) and RCO-ONp( $T_1$ ) were excited to the higher triplet excited states ( $T_n$ ) using the second laser during the two-color two-laser flash photolysis, the C–O-bond cleavage occurred. The C–O-bond cleavage quantum yield ( $\Phi$ )

was estimated from the plots of the  $T_1$ -state esters disappeared within a laser flash versus the second laser intensities. The C–O-bond cleavage in  $^{\beta}$ NpCO-OPh( $T_n$ ) occurred more efficiently than in  $^{\alpha}$ NpCO-OPh( $T_n$ ) and that in PhCO-O $^{\beta}$ Np( $T_n$ ) occurred more efficiently than in PhCO-O $^{\alpha}$ Np( $T_n$ ). The  $\Phi$  value for ester with Ph and  $\beta$ -Np groups was larger than that for ester with Ph and  $\alpha$ -Np groups. The  $\Phi$  value for MeCO-O $^{\alpha}$ Np( $T_n$ ) was similar to those for PhCO-ONp( $T_n$ ), while that

for MeCO-O $^{\beta}$ Np( $T_n$ ) was much smaller than those for PhCO-ONp( $T_n$ ) and MeCO-O $^{\alpha}$ Np( $T_n$ ). On the other hand, no C–O-bond cleavage was observed in NpCO-OMe( $T_n$ ). The  $\Phi$  value depended on the characters of the groups (Np, Ph, and Me) on the ester. Whether R is Ph or Me with or without  $\pi$  electron, respectively, is important for the C–O-bond cleavage. In other words, electronic delocalization of the  $T_n$  state including Np and ester groups is necessary for the occurrence of the C–O-bond cleavage in NpCO-OR( $T_n$ ) and RCO-ONp( $T_n$ ).

**Keywords:** esters • flash photolysis • higher triplet excited state • laser chemistry • photochemistry

## Introduction

Free radicals as reactive intermediates have been extensively investigated. The generation and detection of radicals are very important in physics, chemistry, biology, applied science, and technology. Free radicals generated from homolytic bond cleavages can be used practically as radical initiators of polymerization.<sup>[1,2]</sup> Photochemical generation of radicals usually occurs via the precursors in the singlet or triplet lowest excited states ( $S_1$  and  $T_1$ , respectively).<sup>[3,4]</sup> For example, homolytic CH<sub>2</sub>–X-bond cleavage of ArCH<sub>2</sub>X (Ar = aro-

matic groups such phenyl, naphthyl, pyrenyl, etc., X = halogen, carbonates, phosphites, sulfides, etc.) in the  $S_1$  or  $T_1$  excited state has been widely studied.<sup>[4]</sup> The  $S_1$  and  $T_1$  states are not the only reactive excited states for the bond cleavage.<sup>[5]</sup> Bond cleavages of molecules in the higher excited states occur to give the corresponding radicals. For example, formation of carbazolyl radical from carbazole in the highly excited singlet ( $S_n$ ) and triplet ( $T_n$ ) states has been reported using the double excitation method.<sup>[6,7]</sup> Recently, we have also proven the formation of naphthylmethyl radicals from naphthylmethyl–oxygen (C–O) bond cleavage of naphthylmethoxy compounds in the  $T_n$  states by using the stepwise two-laser irradiations.<sup>[8–11]</sup> The occurrence of the C–O-bond cleavage was found to depend on both the excitation energy and crossing between potential surfaces of the  $T_n$  state and the C–O-bond dissociation. The excitation energy dissipation or electronic delocalization of the  $T_n$  state including the C–O bond is important for the bond cleavage. Herein, we report the C–O-bond cleavage of esters having a naphthyl group, such as NpCO-OR and RCO-ONp (Np =  $\alpha$ - and  $\beta$ -

[a] Dr. X. Cai, M. Sakamoto, Dr. M. Fujitsuka, Prof. Dr. T. Majima  
The Institute of Scientific and Industrial Research (SANKEN)  
Osaka University, Mihogaoka 8-1, Ibaraki  
Osaka 567-0047 (Japan)  
Fax: (+81)6-6879-8499  
E-mail: majima@sanken.osaka-u.ac.jp

[b] Dr. M. Yamaji  
Department of Chemistry, Gunma University  
Kiryu, Gunma 376-8515 (Japan)

naphthyl ( $^{\alpha}\text{Np}$  and  $^{\beta}\text{Np}$ , respectively),  $\text{R} = \text{Ph}$  and  $\text{Me}$ ) in the  $\text{T}_n$  states by the two-color two-laser flash photolysis techniques. The substituent effects on the  $\text{C}-\text{O}$ -bond cleavage in the  $\text{T}_n$  states are discussed. Figure 1 shows the structures of the esters substituted by  $\text{Np}$  used in this study.

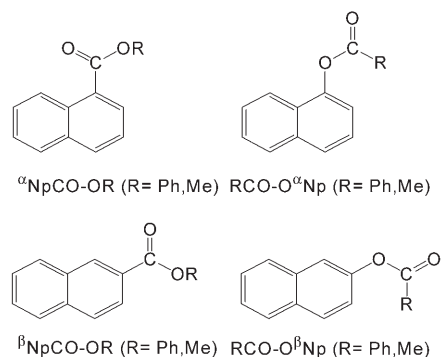


Figure 1. Structures of esters having a naphthyl group ( $\text{Np}$ ) used in this study.

## Results and Discussion

**$\text{C}-\text{O}$ -Bond cleavage of esters with a naphthyl group in the  $\text{S}_1$  state, but not in the  $\text{T}_1$  state:** It is well known that the photo-Fries rearrangement (or [1,3]-shift) reaction occurs following the  $\text{C}-\text{O}$ -bond cleavage of carboxylic acids and their derivatives in the  $\text{S}_1$  state.<sup>[3,12–16]</sup> Therefore, it is expected that the  $\text{C}-\text{O}$ -bond cleavage of esters such as  $\text{NpCO-OR}$  and  $\text{RCO-ONp}$  in the  $\text{S}_1$  state occurs during the laser flash photolysis. The  $\text{C}-\text{O}$ -bond cleavage in  $\text{NpCO-OR}(\text{S}_1)$  and  $\text{RCO-ONp}(\text{S}_1)$  was confirmed by the detection of the transient absorption of the two fragment radicals (Figure 2). For example, the absorption bands of benzoyl radical ( $\text{PhCO}^{\bullet}$ ) and  $\alpha$ -naphthoxy radical ( $^{\alpha}\text{NpO}^{\bullet}$ ) were observed around 325 and 397 nm,<sup>[17–19]</sup> respectively, during the 266 nm laser flash photolysis of  $\text{PhCO-O}^{\alpha}\text{Np}$  (Figure 2e). On the other hand, no  $\text{C}-\text{O}$ -bond cleavage occurred in  $\text{NpCO-OR}(\text{T}_1)$  and  $\text{RCO-ONp}(\text{T}_1)$ . For example, the  $\text{T}_1$ -state transient absorption was observed and decayed during the 355 nm laser flash photolysis of  $\text{PhCO-O}^{\alpha}\text{Np}$  in the presence of benzophenone (BP) used as the triplet sensitizer without formation of any new absorption band (Figure 3e, dotted line). The transient absorption of  $\text{PhCO-O}^{\alpha}\text{Np}(\text{T}_1)$  was similar to that of naphthalene( $\text{T}_1$ ), indicating that the  $\text{T}_1$ -state energy of  $\text{PhCO-O}^{\alpha}\text{Np}(\text{T}_1)$  is localized on the  $\text{Np}$  moiety.<sup>[3,20–22]</sup>

**The  $\text{T}_1$ -state transient absorption:** The transient absorption spectra of the used compounds in the  $\text{T}_1$  state were similar to that of naphthalene( $\text{T}_1$ ) as shown in Figure 3, dotted line. The  $\text{T}_1$ -state transient absorption peaks ( $\lambda_{\text{max}}(\text{T}_1)$ ) and the extinction coefficients of the  $\text{T}_1$ -state transient absorption peaks ( $\epsilon_{\text{max}}$ ) which calculated based on  $\epsilon_{525} = 6250 \text{ M}^{-1} \text{ cm}^{-1}$  of benzophenone( $\text{T}_1$ ) as the reference<sup>[20]</sup> were shown in Table 1.

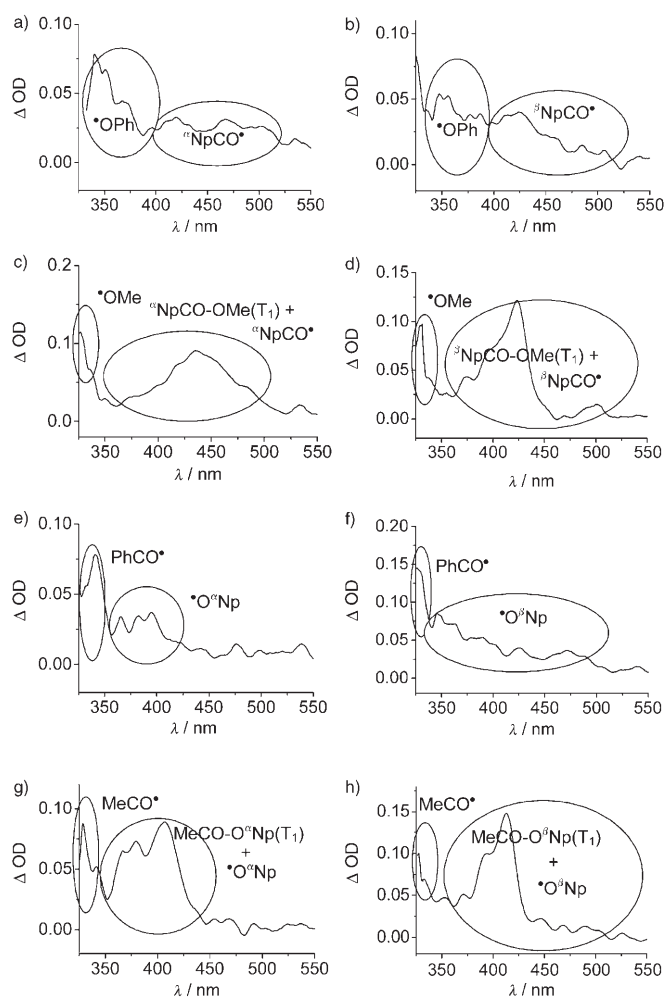


Figure 2. Transient absorption spectra observed during the 266 nm laser flash photolysis of a)  $^{\alpha}\text{NpCO-OPh}$ , b)  $^{\beta}\text{NpCO-OPh}$ , c)  $^{\alpha}\text{NpCO-OMe}$ , d)  $^{\beta}\text{NpCO-OMe}$ , e)  $\text{PhCO-O}^{\alpha}\text{Np}$ , f)  $\text{PhCO-O}^{\beta}\text{Np}$ , g)  $\text{MeCO-O}^{\beta}\text{Np}$ , h) and  $\text{MeCO-O}^{\alpha}\text{Np}$  in argon-saturated acetonitrile at room temperature. The ground-state absorbance of the samples was adjusted to be 1.0 at 266 nm. The transient absorption spectrum was obtained at 100 ns after the 266 nm laser flash. The circles show the absorption positions of the fragment radicals or the  $\text{T}_1$  state.

The  $\lambda_{\text{max}}(\text{T}_1)$  at 460 nm for  $^{\alpha}\text{NpCO-OPh}(\text{T}_1)$ , 426 nm for  $^{\beta}\text{NpCO-OPh}(\text{T}_1)$ , 440 nm for  $^{\alpha}\text{NpCO-OMe}(\text{T}_1)$ , and 422 nm for  $^{\beta}\text{NpCO-OMe}(\text{T}_1)$ , which were broader and shifted to the longer wavelength side compared with that of naphthalene( $\text{T}_1$ ) at 415 nm.<sup>[20]</sup> On the other hand, the  $\lambda_{\text{max}}(\text{T}_1)$  at 405 nm for  $\text{PhCO-O}^{\alpha}\text{Np}(\text{T}_1)$ , 412 nm for  $\text{PhCO-O}^{\beta}\text{Np}(\text{T}_1)$ , 406 nm for  $\text{MeCO-O}^{\alpha}\text{Np}(\text{T}_1)$ , and 412 nm for  $\text{MeCO-O}^{\beta}\text{Np}(\text{T}_1)$ , which were shifted to the shorter wavelength side compared with that of naphthalene( $\text{T}_1$ ) at 415 nm.<sup>[20]</sup> It is suggested that the energy gap ( $\Delta E_{\text{T}_1-\text{T}_n}$ ) between the  $\text{T}_1$  and  $\text{T}_n$  states becomes smaller when  $\text{Np}$  is connected to the carbon atom of the esters,  $\text{NpCO-OR}$ , while it becomes larger when  $\text{Np}$  is connected to the oxygen atom of the esters,  $\text{RCO-ONp}$ . The  $\text{T}_1$ -state transient absorption of esters having a  $\alpha$ - $\text{Np}$  group was broader and shifted to the longer wavelength side compared with those of esters

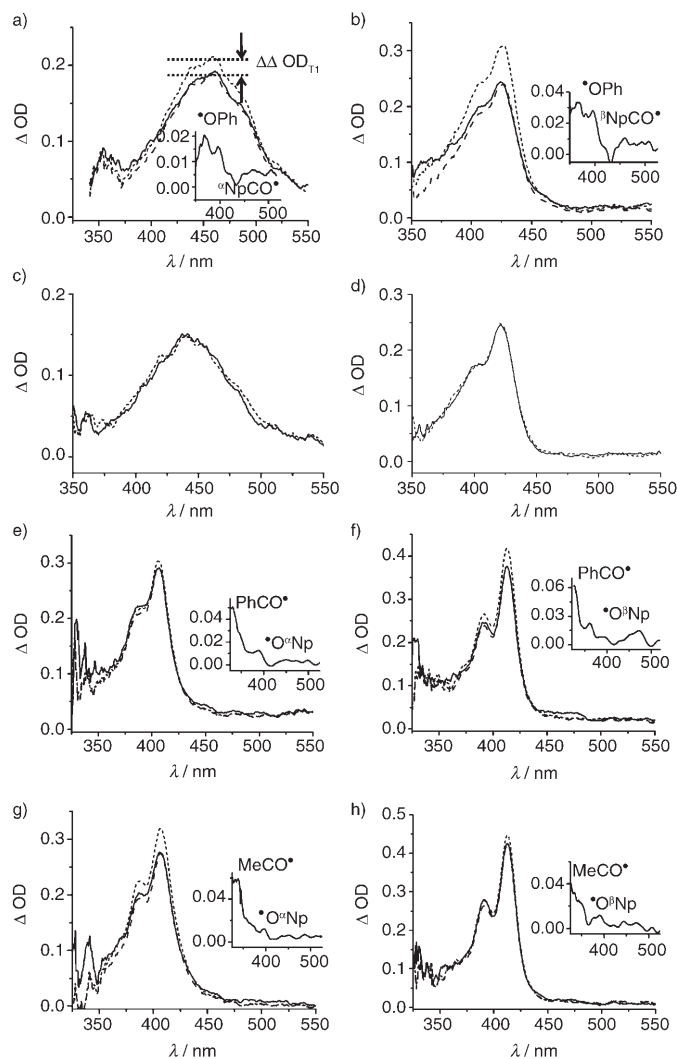


Figure 3. Transient absorption spectra observed during the two-color two-laser flash photolysis of a)  $\alpha$ -NpCO-OPh, b)  $\beta$ -NpCO-OPh, c)  $\alpha$ -NpCO-OMe, d)  $\beta$ -NpCO-OMe, e) PhCO-O $\alpha$ Np, f) PhCO-O $\beta$ Np, g) MeCO-O $\alpha$ Np, h) and MeCO-O $\beta$ Np in argon-saturated acetonitrile ( $6.0 \times 10^{-3}$  M) in the presence of BP ( $6.0 \times 10^{-3}$  M) as the triplet sensitizer. The transient absorption spectra were observed during the 355 nm laser irradiation (at 500 ns after the laser flash) (dotted line) and the successive irradiation with the 355 and 425 nm two-lasers (at 100 ns after the second 425 nm laser flash; delay time between the two lasers, 400 ns) (solid line). The broken lines in a), b), e)–h) were obtained from the transient absorption of the  $T_1$  state multiplied by a factor for OD at the peak fitted to the experimental value, showing the  $T_1$ -state absorption spectra without formation of any new absorption band. Inset, the transient absorption spectra, showing the spectral changes immediately after the second 425 nm laser irradiation, obtained by subtraction of the broken line from the solid line.

having a  $\beta$ -Np group, suggesting that the interaction between the ester moiety and  $\alpha$ -Np is more efficient than for  $\beta$ -Np. In other words, the  $\Delta E_{T_1-T_n}$  is smaller for the esters having a  $\alpha$ -Np group than for those having a  $\beta$ -Np group.

**C–O-Bond cleavage in the  $T_n$  states:** Except for NpCO-OMe( $T_1$ ), the clear depletion of the  $T_1$ -state absorption ( $\Delta\Delta OD$ ) was observed during the second 425 nm laser flash

Table 1.  $T_1$ -state transient absorption peaks ( $\lambda_{\max}(T_1)$ ) and the extinction coefficients of the  $T_1$ -state transient absorption peaks ( $\epsilon_{\max}$ ).

Esters	$\lambda_{\max}(T_1)$ [nm]	$\epsilon_{\max}$ [ $M^{-1}cm^{-1}$ ]
$\alpha$ -NpCO-OPh	460	9380
$\beta$ -NpCO-OPh	426	13800
$\alpha$ -NpCO-OMe	440	6700
$\beta$ -NpCO-OMe	422	10700
PhCO-O $\alpha$ Np	405	13400
PhCO-O $\beta$ Np	412	18300
MeCO-O $\alpha$ Np	406	14300
MeCO-O $\beta$ Np	412	20100

photolysis of NpCO-OR( $T_1$ ) and RCO-ONp( $T_1$ ) (Figure 3, solid line). The  $\Delta\Delta OD$  increased with increasing the 425 nm laser intensity. No recovery of the  $T_1$  state after the second laser flash indicated that decomposition of the  $T_1$  state upon second laser photolysis occurred in the  $T_n$  state.<sup>[8,9,11]</sup> Based on the transient absorption measurement, the decomposition is assigned to the C–O-bond cleavage.<sup>[8,9,11]</sup>

In the case of  $\alpha$ -NpCO-OPh, with a decrease of the absorption intensity of  $\alpha$ -NpCO-OPh( $T_1$ ), absorption bands of phenoxyl radical (PhO $\cdot$ ) at 362 and 398 nm were observed (Figure 3a, solid line).<sup>[17–19]</sup> Absorption bands of the counter radical,  $\alpha$ -naphthoyl radical ( $\alpha$ -NpCO $\cdot$ ) with small and broad peaks in the region of 400–500 nm overlapped with the strong absorption of  $\alpha$ -NpCO-OPh( $T_1$ ). The absorption bands of PhO $\cdot$  around 362 and 398 nm and those of  $\alpha$ -NpCO $\cdot$  in the region of 400–500 nm were obviously observed after subtraction of the broken line, showing that the C–O-bond cleavage occurred from the  $T_n$  state to give  $\alpha$ -NpCO $\cdot$  and PhO $\cdot$  (Figure 3a, inset). Compared with the absorption peak of  $\alpha$ -NpCO-OPh( $T_1$ ) at 460 nm, that of  $\beta$ -NpCO-OPh( $T_1$ ) at 426 nm shifted to the shorter wavelength side. The absorption bands of PhO $\cdot$  around 362 and 398 nm and that of  $\beta$ -naphthoyl ( $\beta$ -NpCO $\cdot$ ) in the region of 450–550 nm were obviously observed after the second 425 nm laser irradiation of  $\beta$ -NpCO-OPh( $T_1$ ) (Figure 3b, inset). Therefore, the C–O-bond cleavage occurred in NpCO-OPh( $T_n$ ) to give PhO $\cdot$  and NpCO $\cdot$  during the two-color two-laser flash photolysis, see Equations (1–3).



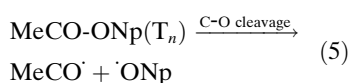
In the case of NpCO-OMe, no depletion of NpCO-OMe( $T_1$ ) was observed during the two-color two-laser flash photolysis (Figure 3c and d), indicating that no C–O-bond cleavage occurred in NpCO-OMe( $T_n$ ).

In the case of PhCO-ONp, appearance of the absorption bands of PhCO $\cdot$  around 325 nm,<sup>[17–19]</sup> and  $\alpha$ -NpO $\cdot$  around 397 nm<sup>[17–19]</sup> or  $\beta$ -NpO $\cdot$  radicals around 382 and 465 nm<sup>[17–19]</sup> were observed during the second 425 nm laser flash photolysis of PhCO-ONp( $T_1$ ) (Figure 3e and f, and insets). The

C–O-bond cleavage occurred in PhCO-ONp( $T_n$ ) during the two-color two-laser flash photolysis, see Equation (4).



In the case of MeCO-ONp, the absorption bands of MeCO $\cdot$  around 340 nm and  $^{\alpha}\text{NpO}^\cdot$  around 397 nm<sup>[17–19]</sup> or  $^{\beta}\text{NpO}^\cdot$  around 382 and 465 nm<sup>[17–19]</sup> were observed during the second 425 nm laser flash photolysis of MeCO-ONp( $T_1$ ) (Figure 3g and h, and insets). The C–O-bond cleavage occurred in MeCO-ONp( $T_n$ ), see Equation (5).



The different  $\Delta\Delta\text{OD}$  values for the different esters during the second 425 nm laser flash photolysis at the same laser intensity indicated the substituent effect on the C–O-bond cleavage in the  $T_n$  states. The  $\Delta\Delta\text{OD}$  value of  $^{\beta}\text{NpCO-OPh}$  was larger than that of  $^{\alpha}\text{NpCO-OPh}$ . That of PhCO-O $^{\beta}\text{Np}$  was larger than that of PhCO-O $^{\alpha}\text{Np}$ . In the case of MeCO-ONp, the  $\Delta\Delta\text{OD}$  value of MeCO-O $^{\alpha}\text{Np}(T_1)$  was larger than that of MeCO-O $^{\beta}\text{Np}(T_1)$ . Effects of the substituent (Ph, Me),  $\alpha$ -Np, and  $\beta$ -Np of the esters on the C–O-bond cleavage are discussed below.

The transient absorption spectra observed during the 266 nm laser flash photolysis of NpCO-OR and RCO-ONp (Figure 2) were essentially equivalent with those observed as new peaks during the two-color two-laser (355 and 425 nm) flash photolysis of NpCO-OR and RCO-ONp (Figure 3, inset). Since same fragment radicals are produced from the  $S_1$  and  $T_n$  states, the C–O-bond cleavage occurs in NpCO-OR( $T_n$ ) and RCO-ONp( $T_n$ ).

**C–O-Bond cleavage quantum yield ( $\Phi$ ) and mechanisms:** It was observed that  $\Delta\Delta\text{OD}$  values increased with increasing the second 425 nm laser intensity. The quantum yields ( $\Phi$ ) of the C–O-bond cleavage in the  $T_n$  states were determined by the procedure reported previously.<sup>[9,10,23]</sup> Figure 4 shows plots of  $\Delta\Delta\text{OD}$  for NpCO-OPh, PhCO-ONp, and MeCO-O $^{\alpha}\text{Np}$  versus the second 425 nm laser intensity. The  $\Phi$  value for MeCO-O $^{\beta}\text{Np}$  was estimated to be less than 0.01 and those for NpCO-OMe were less than 0.001 (Table 2). It is shown that an excited-state energy and a bond dissociation energy are closely correlated and crucial factors for the occurrence of the bond cleavage in the excited states.<sup>[4]</sup> We

have listed the energy levels of the  $S_1$ ,  $T_1$ , and  $T_n$  states ( $E_{S_1}$ ,  $E_{T_1}$ , and  $E_{T_n}$ , respectively) and C–O-bond dissociation energies (BDE) of the compounds used in the present work in Table 2.

Table 2.  $\Phi$  value and the calculated C–O bond dissociation energy (BDE) together with the  $S_1$ -state energy ( $E_{S_1}$ ), the  $T_1$ -state energy ( $E_{T_1}$ ), and the  $T_n$ -state energy ( $E_{T_n}$ ).

Esters	$E_{S_1}^{[a]}$ [kJ mol $^{-1}$ ]	$E_{T_1}^{[a]}$ [kJ mol $^{-1}$ ]	$E_{T_n}^{[b]}$ [kJ mol $^{-1}$ ]	BDE <sup>[c]</sup> [kJ mol $^{-1}$ ]	$\Phi^{[d]}$
$^{\alpha}\text{NpCO-OPh}$	319	240	452	214	0.029
$^{\beta}\text{NpCO-OPh}$	326	241	488	215	0.039
$^{\alpha}\text{NpCO-OMe}$	332	241	452	251	$\leq 0.001$
$^{\beta}\text{NpCO-OMe}$	352	248	490	263	$\leq 0.001$
PhCO-O $^{\alpha}\text{Np}$	362	$\approx 250$	499	191	0.038
PhCO-O $^{\beta}\text{Np}$	359	$\approx 250$	515	211	0.047
MeCO-O $^{\alpha}\text{Np}$	362	249	505	193	0.059
MeCO-O $^{\beta}\text{Np}$	367	243	515	215	< 0.01
MeO-CH $_2^{\alpha}\text{Np}^{[e]}$	366	244	508	256	0.048
MeO-CH $_2^{\beta}\text{Np}^{[e]}$	365	245	509	261	$\leq 0.001$

[a] The  $E_{S_1}$  and  $E_{T_1}$  values of NpCO-OR and RCO-ONp were calculated based on the fluorescence and phosphorescence spectra, respectively. The fluorescence spectra were measured in acetonitrile at 295 K and the phosphorescence spectra were measured in a mixture of methanol-ethanol (1:1 v/v) at 77 K. Because the phosphorescence spectra of PhCO-O $^{\alpha}\text{Np}$  and PhCO-O $^{\beta}\text{Np}$  were absent,  $E_{T_1}$  values of PhCO-O $^{\alpha}\text{Np}$  and PhCO-O $^{\beta}\text{Np}$  were assumed to be equal to those of  $\alpha$ - and  $\beta$ -methoxynaphthalene, respectively.<sup>[20]</sup> [b] The  $E_{T_n}$  values were estimated from the edge of the  $T_1$ -state absorption peak at the longer wavelength side.<sup>[24]</sup> [c] BDE was calculated based on the heat of formation ( $\Delta H_f$ ) for the esters and the fragment radicals using a semi-empirical PM3 program contained in MOPAC'97.<sup>[5]</sup> [d] The quantum yield of the C–O-bond cleavage was calculated from the bleaching of the  $T_1$ -state absorption ( $\Delta\Delta\text{OD}_{T_1}$ ) and the number of the second 425 nm laser photons absorbed by the  $T_1$  state using an actinometry of the T–T absorption of zinc tetraphenylporphyrin at 470 nm in cyclohexane ( $\epsilon_T\Phi_T = 50000 \text{ M}^{-1} \text{ cm}^{-1}$  at 470 nm).<sup>[25]</sup> The data error was in 10%. [e] Ref. [9].

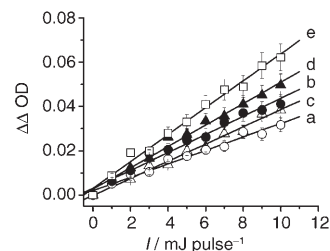


Figure 4. Plots of  $\Delta\Delta\text{OD}_{T_1}$  versus 425 nm laser intensities, a)  $^{\alpha}\text{NpCO-OPh}$  ( $\circ$ ), b)  $^{\beta}\text{NpCO-OPh}$  ( $\bullet$ ), c) PhCO-O $^{\alpha}\text{Np}$  ( $\Delta$ ), d) PhCO-O $^{\beta}\text{Np}$  ( $\blacktriangle$ ), and e) MeCO-O $^{\alpha}\text{Np}$  ( $\square$ ).

Except for  $E_{T_1}$  of NpCO-OMe( $T_1$ ) which is smaller than BDE,  $E_{T_1}$  values of the esters are larger than the corresponding BDE value. Absence of the C–O-bond cleavage in NpCO-OR( $T_1$ ) and RCO-ONp( $T_1$ ) indicates that a large energy barrier ( $\Delta E_{T_1}$ ) exists between the  $T_1(\pi, \pi^*)$  state and the C–O-bond dissociation potential surfaces.<sup>[9,10]</sup> Figure 5. On the other hand, the occurrence of the C–O-bond cleavage in the  $T_n$  state indicates that a small energy barrier ( $\Delta E_{T_n}$ ) exists between the  $T_n$  state and the C–O bond dissociation potential surfaces. During the second 425 nm laser irradiation of the  $T_1$  state, the  $T_n(\pi, \pi^*)$  state is initially produced together with many other  $T_n$  states, having lower excitation energies than that of the  $T_n(\pi, \pi^*)$  state via the rapid internal conversion (IC), from which the C–O-bond cleavage occurs. The electronic delocalization including Np and ester groups must be involved in such  $T_n$  state (reactive  $T_n$



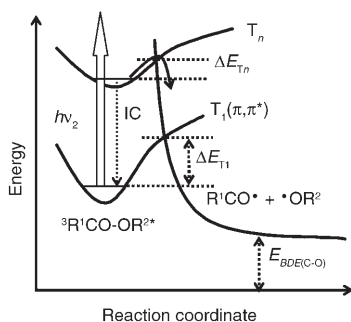


Figure 5. An energy diagram during the C–O-bond cleavage of esters ( $R^1CO-OR^2$ ) during the two-color two-laser flash photolysis;  $h\nu_2$ : the second 425 nm laser excitation, IC: internal conversion,  $\Delta E_{T_1}$ : an energy barrier between the potential surfaces of the  $T_1(\pi, \pi^*)$  state and the C–O bond dissociation,  $\Delta E_{T_n}$ : an energy barrier between the potential surfaces of the  $T_n$  state and the C–O-bond dissociation,  $R^1CO\cdot$  and  $\cdot OR^2$ : the fragment radicals.

state). In other words, the reactive  $T_n$  state has not only  $\pi, \pi^*$  character but also  $\sigma, \sigma^*$  character of the C–O bond. Therefore, this reactive  $T_n$  state correlates with the C–O-bond dissociation potential surface leading to the C–O-bond cleavage. Accordingly, absence of C–O-bond cleavage in  $NpCO-OMe(T_n)$ , indicates that  $\Delta E_{T_n}$  for  $NpCO-OMe$  is very large.

**Substituent effects on the C–O-bond cleavage:** For the occurrence of the C–O-bond cleavage in the  $T_n$  state, three key factors are probably considered. Firstly, the  $E_{T_n}$  should be larger than BDE. Secondly, since the C–O-bond cleavage in the  $T_n$  state is a competitive process with the internal conversion from the  $T_n$  state to the  $T_1$  state,<sup>[8,9,11]</sup> the lifetime of the  $T_n$  state must be enough long to correlate with a dissociative potential surface leading to the C–O-bond cleavage. Thirdly, the electronic delocalization in the  $T_n$  state is necessary for the occurrence of the C–O-bond cleavage. The data in Table 2 show that all  $E_{T_n}$  values are much larger than BDEs, suggesting that the  $E_{T_n}$  must be a key factor, but not the most important one for the occurrence of the C–O-bond cleavage in the  $T_n$  state.

For the second factor, the lifetimes of several substituted naphthalenes in the  $T_n$  states have been reported in a time domain of several tens picoseconds.<sup>[22]</sup> Since the  $T_1$ -state energy is mainly localized on the Np moiety, the  $NpCO-OR$  and  $RCO-ONp$  esters can be identified as the substituted naphthalenes. The  $T_n$ -state lifetimes of  $NpCO-OR(T_n)$  and  $RCO-ONp(T_n)$  are expected to be similar to those of the reported substituted naphthalenes (10–60 ps). Since the C–O-bond cleavage occurs in the fs–ps time scale in the ground and excited states,<sup>[3,4,14]</sup> such lifetimes of 10–60 ps for the  $T_n$  states would be enough long for the occurrence of the C–O-bond cleavage.

For the third factor, it is very important whether the C–O bond is involved in the electronic delocalization in  $NpCO-OR(T_n)$  or  $RCO-ONp(T_n)$ , and it is clear that R,  $\alpha$ -Np, and  $\beta$ -Np have serious effects. In the case of  $NpCO-OPh$ , the

electronic delocalization in  $NpCO-OPh(T_n)$  including Ph is possible because of the  $\pi$  electrons of Ph. On the other hand, such electronic delocalization in  $NpCO-OMe(T_n)$  including Me is impossible because of no  $\pi$  electron of Me. Therefore, whether R is Ph or Me with or without  $\pi$  electrons, respectively, is important for the occurrence of the C–O-bond cleavage in  $NpCO-OR(T_n)$ . In the case of  $NpCO-OPh$ , the broad and red-shifted absorption of  ${}^{\alpha}NpCO-OPh(T_1)$  compared with that of  ${}^{\beta}NpCO-OPh(T_1)$  was observed. The  $\Delta E_{T_1-T_n}$  of  ${}^{\alpha}NpCO-OPh$  is smaller than that of  ${}^{\beta}NpCO-OPh$ . Since the C–O-bond cleavage in the  $T_n$  state is a competitive process with the internal conversion from the  $T_n$  state to the  $T_1$  state, the  $\Phi$  of the C–O-bond cleavage in the  $T_n$  state should depend on the  $T_n$ -state lifetime. The  $T_n$ -state lifetime and the relationship with the  $\Delta E_{T_1-T_n}$  value have been reported for the substituted naphthalenes in the  $T_n$  states.<sup>[22]</sup> The smaller  $\Delta E_{T_1-T_n}$  value corresponds to the shorter lifetime of the  $T_n$ -state and the faster internal conversion from the  $T_n$  to  $T_1$  states. Consequently, the  $\Phi$  of the C–O-bond cleavage in  ${}^{\alpha}NpCO-OPh(T_n)$  is expected to be smaller than that of  ${}^{\beta}NpCO-OPh(T_n)$ .

Similar to  $NpCO-OPh(T_n)$ , the electronic delocalization between Np and Ph moieties in  $PhCO-ONp(T_n)$  is possible because of  $\pi$  electrons of Ph. The broader and red-shifted absorption of  $PhCO-O^{\alpha}Np(T_1)$  than that of  $PhCO-O^{\beta}Np(T_1)$  indicates that the  $\Delta E_{T_1-T_n}$  of  $PhCO-O^{\alpha}Np$  is smaller than that of  $PhCO-O^{\beta}Np$ . Consequently, the  $\Phi$  of the C–O-bond cleavage in  $PhCO-O^{\alpha}Np(T_n)$  is expected to be smaller than that of  $PhCO-O^{\beta}Np(T_n)$ .

On the other hand, in the case of  $MeCO-ONp$  and  $NpCO-OMe$ , such electronic delocalization in  $MeCO-ONp(T_n)$  and  $NpCO-OMe(T_n)$  including Np and Me moieties is impossible because of no  $\pi$  electron of Me. Therefore, the mechanism of the occurrence of the C–O-bond cleavage in  $MeCO-ONp(T_n)$  is different from those in  $PhCO-ONp(T_n)$  and  $NpCO-OPh(T_n)$ . In the case of  $MeCO-ONp$ , the C–O-bond cleavage mechanism could be similar to that of methoxymethylnaphthalene ( $MeO-CH_2Np$ ).<sup>[8,9,11]</sup> The  $\Phi$  value of the C–O-bond cleavage in  $MeO-CH_2^{\alpha}Np(T_n)$  was 0.048, while no C–O-bond cleavage occurred in  $MeO-CH_2^{\beta}Np(T_n)$ . The different  $\Phi$  values for  $MeO-CH_2^{\alpha}Np$  and  $MeO-CH_2^{\beta}Np$  should be due to the electronic character and conformation difference for  $\alpha$ -Np and  $\beta$ -Np. Because the methyl carbon of  $CH_2Np$  is  $sp^3$  carbon atom, the  $\sigma$  C–O bond can interact with  $\pi$  electrons of Np. Such interaction is expected to be larger in  $MeO-CH_2^{\alpha}Np(T_n)$  than that in  $MeO-CH_2^{\beta}Np(T_n)$  because of the different substitution positions of the  $sp^3$  carbon atom in  $MeO-CH_2Np(T_n)$ . Consequently, the C–O-bond cleavage occurs in  $MeO-CH_2^{\alpha}Np(T_n)$ , but not in  $MeO-CH_2^{\beta}Np(T_n)$ .

The  $sp^3$  carbon atom connects on Np in  $MeO-CH_2Np$ , while the  $sp^3$  oxygen atom connects on Np in  $MeCO-ONp$ . Since the  $sp^3$  oxygen atom has non-bonding electrons, the interaction between the  $\sigma$  C–O bond and Np moiety in  $MeCO-ONp$  is expected to be stronger than that in  $MeO-CH_2Np$ . Therefore, the  $\sigma$  C–O-bond cleavage occurs more efficiently in  $MeCO-ONp(T_n)$  than in  $MeO-CH_2Np(T_n)$ .

( $\Phi = 0.059$ ,  $< 0.01$ ,  $0.048$ , and  $\ll 0.001$  for  $\text{MeCO-O}^\alpha\text{Np}$ ,  $\text{MeCO-O}^\beta\text{Np}$ ,  $\text{MeO-CH}_2^\alpha\text{Np}$ , and  $\text{MeO-CH}_2^\beta\text{Np}$ , respectively, Table 2). Such electronic interaction is expected to be more efficient in  $\text{MeO-CH}_2^\alpha\text{Np}(T_n)$  and  $\text{MeCO-O}^\alpha\text{Np}(T_n)$  than in  $\text{MeO-CH}_2^\beta\text{Np}(T_n)$  and  $\text{MeCO-O}^\beta\text{Np}(T_n)$ , because of the different substitution positions of the  $\text{sp}^3$  carbon and oxygen atoms in  $\text{MeO-CH}_2^\alpha\text{Np}(T_n)$  and  $\text{MeCO-O}^\alpha\text{Np}(T_n)$ , respectively.

The electronic interaction between Ar and R moieties involving the C–O bond of  $\text{ArCO-OR}$  (Ar = Ph, R = Np, or Ar = Np, R = Ph) in the  $T_n$  states causes the C–O-bond cleavage. Although the  $T_1$  state is localized on Np moiety, the  $T_n$  state could be delocalized on Np and Ar moieties including the C–O bond in  $\text{ArCO-OR}(T_n)$ . Therefore, the C–O bond has the antibonding character, leading to the C–O-bond cleavage. On the other hand, in the cases of  $\text{NpCO-OMe}$ ,  $\text{MeCO-ONp}$ , and  $\text{MeO-CH}_2\text{Np}$ , the C–O-bond cleavage depends on the interaction between the  $T_n$  state of Np and the antibonding orbital of the C–O bond. In  $\text{NpCO-OMe}$ , the  $T_1$  state of Np is delocalized including the carboxy group (NpCO moiety), based on the broad and red-shifted absorption of the  $T_1$  state (Figure 3c and d). The  $T_n$  state of the planar NpCO moiety can not interact electronically with the C–O bond, because the C–O bond orbital is almost perpendicular to the  $\pi$  electronic orbital of the NpCO moiety or the interaction between the C–O-bond orbital and the  $\pi$ -electronic orbital of the NpCO moiety is negligible. Therefore, no C–O-bond cleavage occurs in  $\text{NpCO-OMe}(T_n)$ . In  $\text{MeCO-ONp}$  and  $\text{MeO-CH}_2\text{Np}$ , the  $T_n$ -state orbital of Np can not strongly interact with the C–O bond because of no  $\pi$  electron of Me group, but weakly interact with the C–O bond. Therefore, the C–O bond has some antibonding character, and the  $\Phi$  values of the C–O-bond cleavage are small in  $\text{MeCO-ONp}(T_n)$  and  $\text{MeO-CH}_2\text{Np}(T_n)$ .

The obvious effects of  $\alpha$ - and  $\beta$ -Np on the C–O-bond cleavage in  $\text{MeCO-ONp}(T_n)$  and  $\text{MeO-CH}_2\text{Np}(T_n)$  should be due to the difference of the electronic interaction between the  $\sigma$  C–O bond and the  $\alpha$ - and  $\beta$ -Np moieties. It is known that absorption of naphthalene( $T_1$ ) is due to two transitions, the short-axis polarized transition ( ${}^3A_{1g}^- \leftarrow {}^3B_{2u}^+$ ) and the long-axis polarized transition ( ${}^3B_{3g}^- \leftarrow {}^3B_{2u}^+$ ).<sup>[26–28]</sup> In  $\alpha$ -Np, the short-axis polarized transition ( ${}^3A_{1g}^- \leftarrow {}^3B_{2u}^+$ ) is enhanced, the absorption of  $\alpha$ -Np( $T_1$ ) becomes broader and red-shifted than that of naphthalene( $T_1$ ), while in  $\beta$ -Np, the long-axis polarized transition ( ${}^3B_{3g}^- \leftarrow {}^3B_{2u}^+$ ) is enhanced. The absorption of  $\beta$ -Np( $T_1$ ) resembles that of naphthalene( $T_1$ ).<sup>[22,26–28]</sup> It is suggested that the electronic delocalization in  $\alpha$ -Np( $T_1$ ) is larger than that in  $\beta$ -Np( $T_1$ ). Such larger electronic delocalization is expected in  $\alpha$ -Np( $T_n$ ) than that in  $\beta$ -Np( $T_n$ ). Because of this electronic delocalization difference in  $\alpha$ -Np( $T_n$ ) and  $\beta$ -Np( $T_n$ ), the more interaction between the  $\sigma$  C–O bond and Np moiety in  $\text{MeO-CH}_2^\alpha\text{Np}(T_n)$  and  $\text{MeCO-O}^\alpha\text{Np}(T_n)$  than that in  $\text{MeO-CH}_2^\beta\text{Np}(T_n)$  and  $\text{MeCO-O}^\beta\text{Np}(T_n)$  is reasonable. The C–O bond has more antibonding character in  $\text{MeO-CH}_2^\alpha\text{Np}(T_n)$  and  $\text{MeCO-O}^\alpha\text{Np}(T_n)$  than in  $\text{MeO-CH}_2^\beta\text{Np}(T_n)$  and  $\text{MeCO-O}^\beta\text{Np}(T_n)$ . Therefore, the C–O-bond cleavage occurs

more efficiently in  $\text{MeO-CH}_2^\alpha\text{Np}(T_n)$  and  $\text{MeCO-O}^\alpha\text{Np}(T_n)$  than in  $\text{MeO-CH}_2^\beta\text{Np}(T_n)$  and  $\text{MeCO-O}^\beta\text{Np}(T_n)$ .<sup>[9]</sup>

The electronic interaction between Np and R moieties involving the C–O bond of  $\text{NpCO-OR}$  and  $\text{RCO-ONp}$  also causes a change of the BDE value. The BDE values of  $\text{NpCO-OR}$  and  $\text{RCO-ONp}$ , R = Ph with  $\pi$  electrons, are smaller than those of R = Me without  $\pi$  electrons (Table 2). A relationship between the BDE versus  $\Phi$  values indicates that the smaller BDE value correlates to the larger  $\Phi$  value (Figure 6). In another words, the large electronic interaction between Np and R moieties of  $\text{NpCO-OR}(T_n)$  and  $\text{RCO-ONp}(T_n)$  leads to the small BDE value and the large  $\Phi$  value.

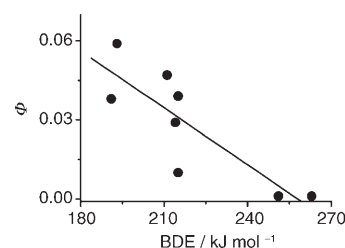


Figure 6. Plots of  $\Phi$  versus BDE values of esters in Table 2.

## Conclusion

C–O-Bond cleavage of several esters in the  $T_n$  states was observed during the two-color two-laser flash photolysis at room temperature. The quantum yields ( $\Phi$ ) of the C–O-bond cleavage were estimated based on the plots of the disappeared  $T_1$  state versus the second 425 nm laser intensities and listed in Table 2. The  $\Phi$  value seems to depend on the characters of the substituent groups on the esters. The C–O-bond cleavage in  ${}^\beta\text{NpCO-OPh}(T_n)$  occurred more efficiently than in  ${}^\alpha\text{NpCO-OPh}(T_n)$  and that in  $\text{PhCO-O}^\beta\text{Np}(T_n)$  occurred more efficiently than in  $\text{PhCO-O}^\alpha\text{Np}(T_n)$ . In the case of  $\text{MeCO-ONp}$ , the  $\Phi$  value for  $\text{MeCO-O}^\alpha\text{Np}(T_n)$  was larger than that for  $\text{MeCO-O}^\beta\text{Np}(T_n)$ . No C–O-bond cleavage occurred in  $\text{NpCO-OMe}(T_n)$ . The electronic delocalization in the  $T_n$  state is necessary for the occurrence of the C–O-bond cleavage in  $\text{NpCO-OR}(T_n)$  or  $\text{RCO-ONp}(T_n)$ . Therefore, R, Ph or Me with or without  $\pi$  electrons, respectively, is one of key factors for the occurrence of the C–O-bond cleavage in the  $T_n$  states. When R is Ph with  $\pi$  electrons, the C–O bond is involved in the electronic delocalization between Ph and Np moieties in the  $T_n$  state, resulting in the occurrence of the C–O-bond cleavage in  $\text{NpCO-OPh}(T_n)$  and  $\text{PhCO-ONp}(T_n)$ . In the case of  $\text{NpCO-OMe}(T_n)$  and  $\text{MeCO-ONp}(T_n)$ , R is Me without  $\pi$  electrons, the C–O-bond cleavage depends strongly on the electronic interaction between the C–O bond and Np moiety. The larger electronic interaction in  $\text{MeCO-O}^\alpha\text{Np}(T_n)$  than in  $\text{MeCO-O}^\beta\text{Np}(T_n)$  results in the  $\Phi$  value larger for  ${}^\alpha\text{Np}$  compounds( $T_n$ ) than for  ${}^\beta\text{Np}$  compounds( $T_n$ ).

## Experimental Section

**Materials:**  $\alpha$ - and  $\beta$ -Naphthoyl phenyl esters ( $^{14}\text{C}$ -NpCO-OPh and  $^{14}\text{C}$ -NpCO-OPh) and  $\alpha$ - and  $\beta$ -naphthoyl methyl esters ( $^{14}\text{C}$ -NpCO-OMe and  $^{14}\text{C}$ -NpCO-OMe) were synthesized by reactions of naphthoyl chloride with phenol and methanol, respectively. Benzoyl  $\alpha$ - and  $\beta$ -naphthyl esters (PhCO- $^{14}\text{C}$ -Np and PhCO- $^{14}\text{C}$ -Np) and acetyl  $\alpha$ - and  $\beta$ -naphthyl esters (MeCO- $^{14}\text{C}$ -Np and MeCO- $^{14}\text{C}$ -Np) were synthesized by reaction of  $\alpha$ - and  $\beta$ -naphthol with benzoic anhydride and acetic anhydride, respectively. Benzophenone from Nacalai Tesque Inc was purified from ethanol before use as the triplet sensitizer. Acetonitrile (spectral grade) from Nacalai Tesque Inc was used as received. All sample solutions were freshly prepared and deoxygenated by bubbling with argon before irradiation. The ground-state absorbance of the naphthyl derivatives was adjusted to be 1.0 at 266 nm during the 266 nm laser flash photolysis. BP ( $6.0 \times 10^{-3}\text{ M}$ ) and naphthyl derivatives ( $6.0 \times 10^{-3}\text{ M}$ ) were used during the two-color two-laser flash photolysis. All experiments were carried out at room temperature.

**Two-color two-laser flash photolysis:** Third and fourth harmonics (355 and 266 nm, respectively) from a Nd:YAG laser (Brilliant, Quantel; 5 ns full width at half maximum (fwhm)) and the laser light at 425 nm ( $7\text{ mJ pulse}^{-1}$ ) from an OPO laser (Continuum, Surelite OPO) which was pumped by another Nd:YAG laser (Continuum, Surelite II-10; 5 ns fwhm) were used as excitation light sources. Two laser flashes were synchronized by a pulse generator with a delay time of 10 ns–10  $\mu\text{s}$ . The probe light was obtained from a 450 W Xe lamp (Osram XBO-450). The transmitted probe light was focused on a monochromator (Nikon G250). The output of the monochromator was monitored using a photomultiplier tube (PMT, Hamamatsu Photonics, R928). The signal from the PMT was recorded on a transient digitizer (Tektronix TDS 580D). A multichannel analyzer system (Hamamatsu Photonics, C5967) was used for the measurement of the transient absorption spectra. The total system was controlled with a personal computer via GP-IB interface. To avoid any damage of the sample solution by the probe light, a suitable cutoff filter was used in front of the sample. The eight time shots to one sample at each wavelength were carried out to get one set of experimental data, and then the sample was replaced by the fresh one. The experiments were carried out three times.

## Acknowledgements

This work has been partly supported by a Grant-in-Aid for Scientific Research (Project 17105005, Priority Area (417), 21st Century COE Research, and others) from the Ministry of Education, Culture, Sports, Science and Technology (MEXT) of Japanese Government. The authors also thank to JSPS for a fellowship for X.C.

- [1] S. N. Gupta, I. Gupta, D. C. Neckers, *J. Polym. Sci. Polym. Chem. Ed.* **1981**, *19*, 103.  
[2] B. K. Shah, D. C. Neckers, *J. Org. Chem.* **2002**, *67*, 6117.

- [3] N. J. Turro, *Modern Molecular Photochemistry*, The Benjamin/Cummings Publishing, Menlo Park, California, **1978**.  
[4] S. A. Fleming, J. A. Pincock, *Mol. Supramol. Photochem.* **1999**, *3*, 211.  
[5] M. Yamaji, T. Yoshihara, T. Tachikawa, S. Tero-Kubota, S. Tobita, H. Shizuka, B. Marciniak, *J. Photochem. Photobiol. A* **2004**, *162*, 513.  
[6] S. Yamamoto, K. Kikuchi, H. Kokubun, *Chem. Lett.* **1977**, 1173.  
[7] M. Martin, E. Breheret, F. Tfibel, B. Lacourbas, *J. Phys. Chem.* **1980**, *84*, 70.  
[8] X. Cai, M. Sakamoto, M. Hara, S. Tojo, M. Fujitsuka, A. Ouchi, T. Majima, *Chem. Commun.* **2003**, 2604.  
[9] X. Cai, M. Sakamoto, M. Hara, S. Tojo, A. Ouchi, A. Sugimoto, K. Kawai, M. Endo, M. Fujitsuka, T. Majima, *J. Phys. Chem. A* **2005**, *109*, 3797.  
[10] X. Cai, M. Sakamoto, M. Yamaji, M. Fujitsuka, T. Majima, *J. Phys. Chem. A* **2005**, *109*, 5989.  
[11] X. Cai, M. Sakamoto, M. Hara, S. Tojo, A. Ouchi, K. Kawai, M. Endo, M. Fujitsuka, T. Majima, *J. Am. Chem. Soc.* **2004**, *126*, 7432.  
[12] C. E. Kalmus, D. M. Hercules, *J. Am. Chem. Soc.* **1974**, *96*, 449.  
[13] M. A. Miranda, F. Galindo, *CRC Handbook of Organic Photochemistry and Photobiology*, 2nd ed., **2004**, Chapter 42, pp. 1–11.  
[14] S. Lochbrunner, M. Zissler, J. Piel, E. Riedle, A. Spiegel, T. Bach, *J. Chem. Phys.* **2004**, *120*, 11634.  
[15] S. Koodanjeri, A. R. Pradhan, L. S. Kaanumalle, V. Ramamurthy, *Tetrahedron Lett.* **2003**, *44*, 3207.  
[16] I. F. Molokov, Y. P. Tsentalovich, A. V. Yurkovskaya, R. Z. Sagdeev, *J. Photochem. Photobiol. A* **1997**, *110*, 159.  
[17] A. Habersbergerova, I. Janovsky, J. Teply, *Radiat. Res. Rev.* **1968**, *1*, 109.  
[18] A. Habersbergerova, I. Janovsky, P. Kourim, *Radiat. Res. Rev.* **1972**, *4*, 123.  
[19] M. Y. Melnikov, V. A. Smirnov, *Handbook of Photochemistry of Organic Radicals: Absorption and Emission Properties, Mechanisms, Aging*, Begell House, New York, Wallingford (UK), **1996**.  
[20] S. L. Murov, I. Carmichael, G. L. Hug, *Handbook of Photochemistry*, Marcel Dekker, New York, **1993**.  
[21] M. Sakamoto, X. Cai, M. Hara, S. Tojo, M. Fujitsuka, T. Majima, *J. Phys. Chem. A* **2004**, *108*, 10941.  
[22] M. Sakamoto, X. Cai, M. Hara, M. Fujitsuka, T. Majima, *J. Phys. Chem. A* **2005**, *109*, 4657.  
[23] X. Cai, M. Sakamoto, M. Hara, S. Inomata, M. Yamaji, S. Tojo, K. Kawai, M. Endo, M. Fujitsuka, T. Majima, *Chem. Phys. Lett.* **2005**, *407*, 402.  
[24] M. Sakamoto, X. Cai, M. Hara, M. Fujitsuka, T. Majima, *J. Am. Chem. Soc.* **2004**, *126*, 9709.  
[25] A. Ishida, M. Fukui, H. Ogawa, S. Tojo, T. Majima, S. Takamuku, *J. Phys. Chem.* **1995**, *99*, 10808.  
[26] L. Klasinc, U. Sommer, *Chem. Phys. Lett.* **1969**, *3*, 107.  
[27] D. Lavalette, *Chem. Phys. Lett.* **1969**, *3*, 264.  
[28] T. G. Pavlopoulos, *Chem. Phys. Lett.* **1973**, *20*, 207.

Received: June 12, 2006  
Published online: January 10, 2007